

# Galaxy clustering in the Legacy Survey and its imprint on the CMB

Qianjun (Ellen) Hang, Edinburgh University

Supervisors:

Shadab Alam, John Peacock, Yan-Chuan Cai

21 October 2020 DESI Lunch @ LBL



European Research Council  
Established by the European Commission

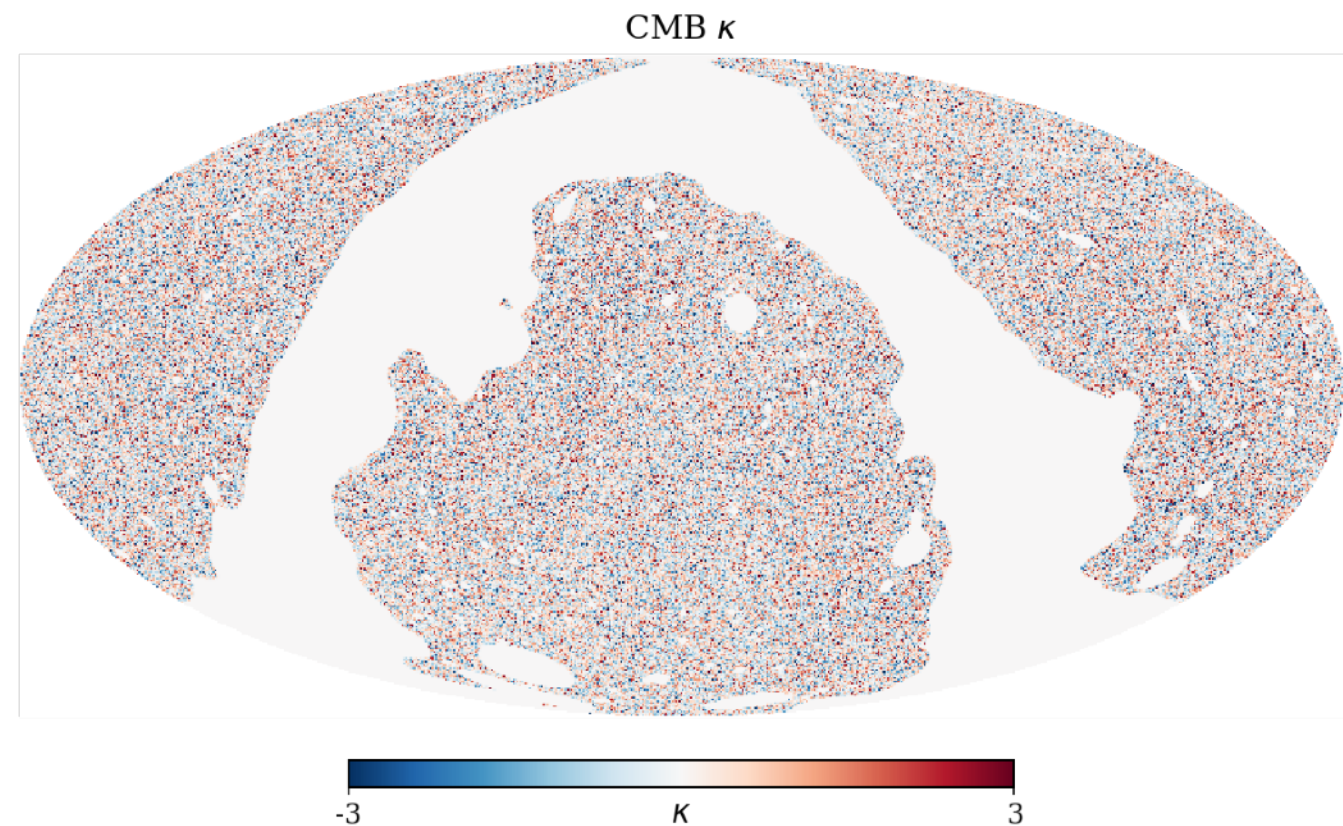
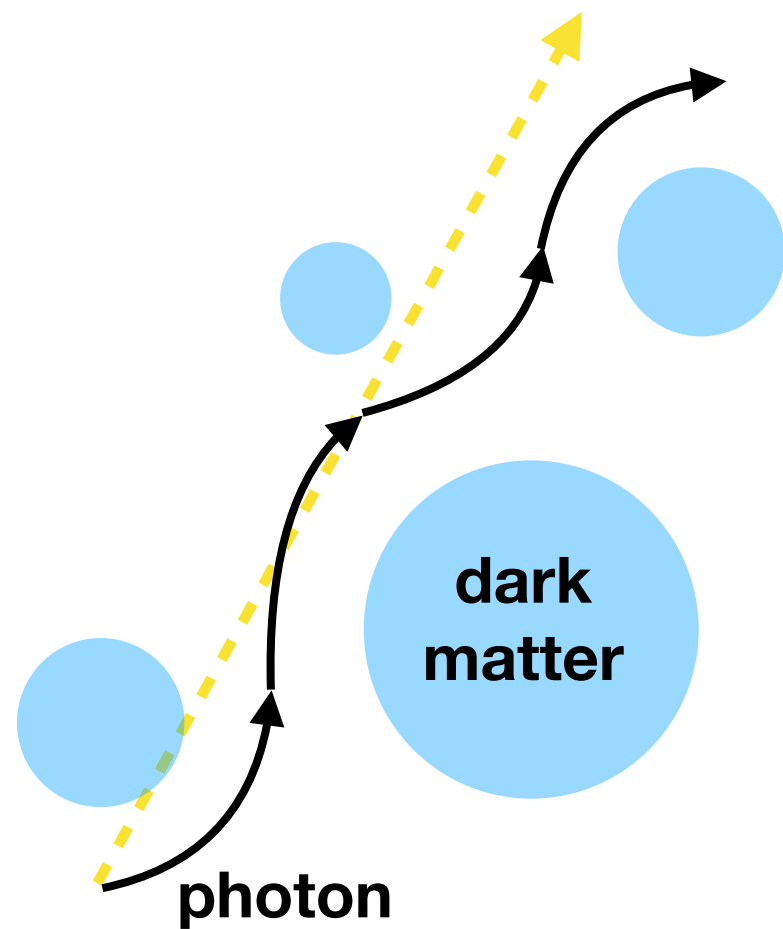


Q. Hang et al 2020, arXiv: 2010.00466

# I will talk about...

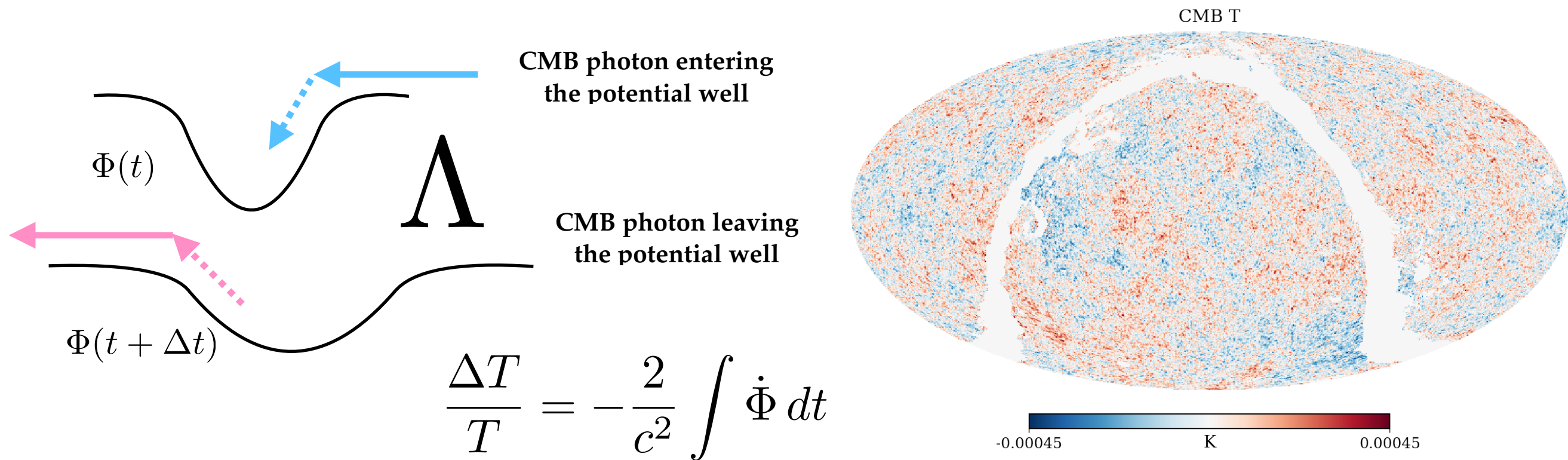
1. Motivation and theory
2. Legacy Survey and selection
3. Calibration of the photometric redshifts
4. Cross-correlation Results and errors
5. Conclusion: a lower-density universe

# Imprints on the CMB lensing map



- Weak gravitational lensing  $\rightarrow$  deflect CMB photon trajectory by LSS
- Distortion on the CMB  $\rightarrow$   $\kappa$  map
- Matter density projected along the line of sight from the CMB to us.

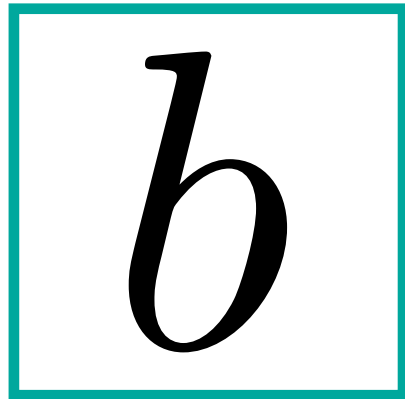
# Imprints on the CMB temperature map



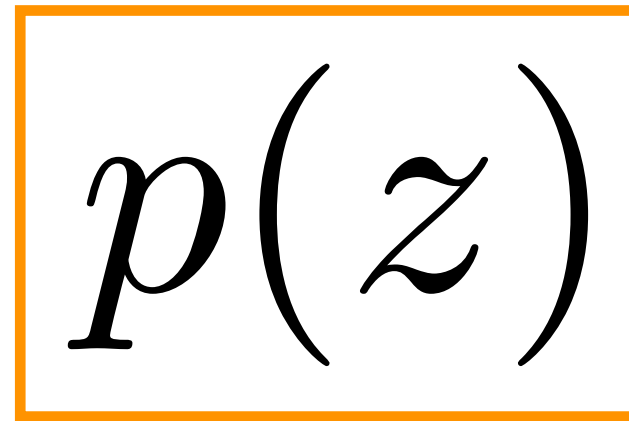
- Integrated Sachs-Wolfe (ISW) → energy shifts in the CMB photons due to LSS
- Only present with the late time dark energy domination → time-varying potential.
- Modifies the peaks and troughs in the CMB temperature fluctuations. Power mostly on large scales.

Aim: measure this signal \*tomographically\* by cross-correlating with galaxies in redshift bins

# galaxy-galaxy auto/cross-correlations between redshift slices


$$b$$

- Galaxies are biased tracers of matter,  $\delta_g = b\delta_m$
- Constraint by galaxy auto-correlations
- (Data)/(Theory with dark matter) =  $b^2$ .


$$p(z)$$

- Photometric redshift distribution is uncertain
- Constraint by galaxy cross-correlations
- Bias independent correlation coefficient:

$$r = \frac{C_\ell^{AB}}{\sqrt{C_\ell^{AA} C_\ell^{BB}}}$$

# Methods

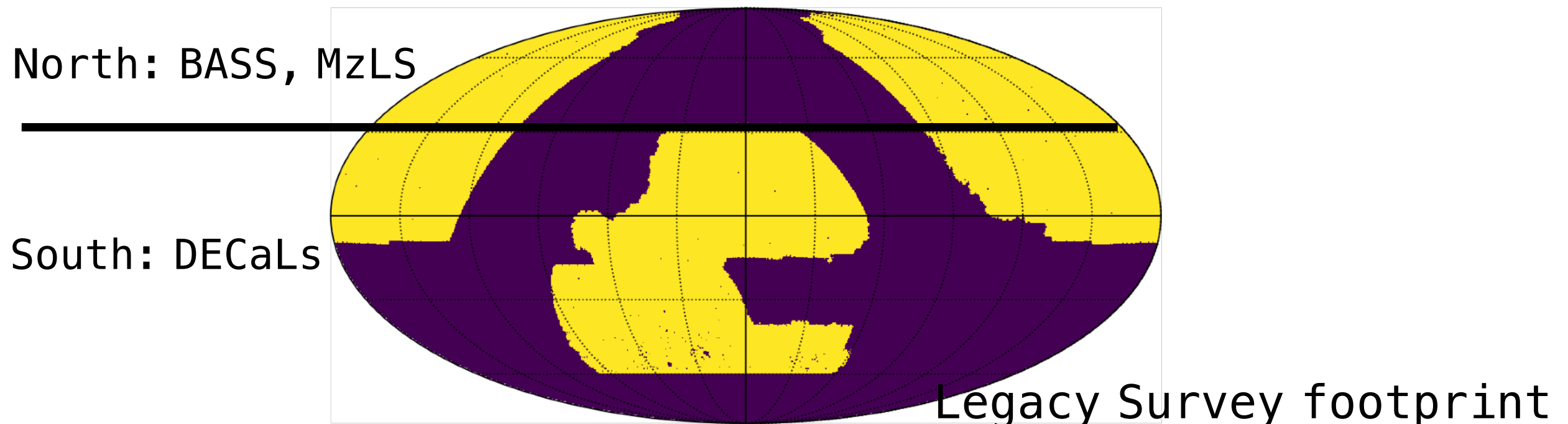
- Measurement: **Healpy (Healpix)**  $\rightarrow$  pixellated map  $\rightarrow$  spherical harmonics,  $a_{\ell m}$   $\rightarrow$  Angular power spectrum  $C_\ell$
- Maps: **Planck 2018** lensing convergence and temperature maps with masks.
- Theory: non-linear matter power spectrum from **CAMB** (**halofit** for the non-linear part)
- Fiducial Cosmology: Planck 2018 best-fit parameters

$$\boxed{\Omega_m = 0.315 \quad \sigma_8 = 0.811} \quad h = 0.674$$

$$n_s = 0.965 \quad \Omega_b = 0.0493$$

# 2. Legacy Survey and selection

- The DESI Legacy Imaging Survey (DR7) covers an area of  $14,000 \text{ deg}^2$ , about **1/3 of the whole sky**, with  $\sim 0(10^8)$  galaxies. It's a combination of **3 telescopes**: DECaLS in the south and BASS+MzLS in the north.
- The photometric bands available are: **g, r, z** (optical wavelength), and three WISE bands: **W1, W2, W3** (infrared wavelength).
- It is really amazing that DESI made this great dataset **public** for the world community!



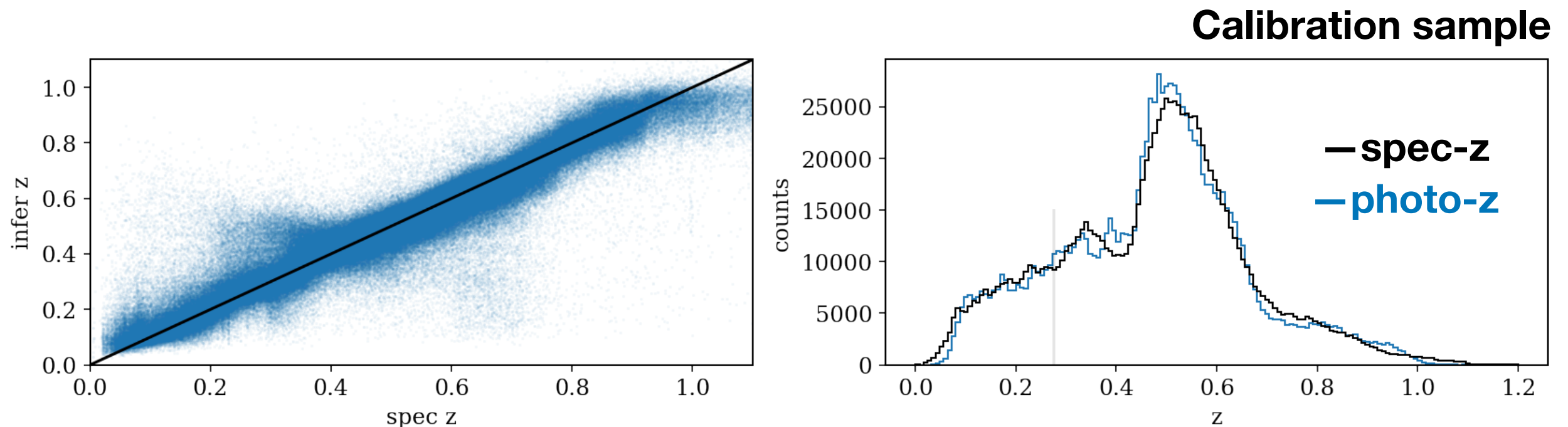
# 2. Legacy Survey and selection

- Exclude PSF types (*stars, quasars etc.*);
- Require measurements in g, r, z, and w1 bands;
- Apply *galactic extinction* correction;
- *Magnitude cuts*:  $g < 24$ ,  $r < 22$ ,  $w1 < 19.5$  for uniform depth;
- *Completeness map* from Bitmask: pixels  $> 0.86$   $\rightarrow$  weights; pixels  $< 0.86$   $\rightarrow$  masked.
- Normalize North and South separately;
- We correct for *stellar density* from the ALLWISE total density map (very large scales near galactic plane) [more](#);
- Selection based on 3D colour (see next slide).

$\sim 4.5 \times 10^7$   
galaxies  
selected

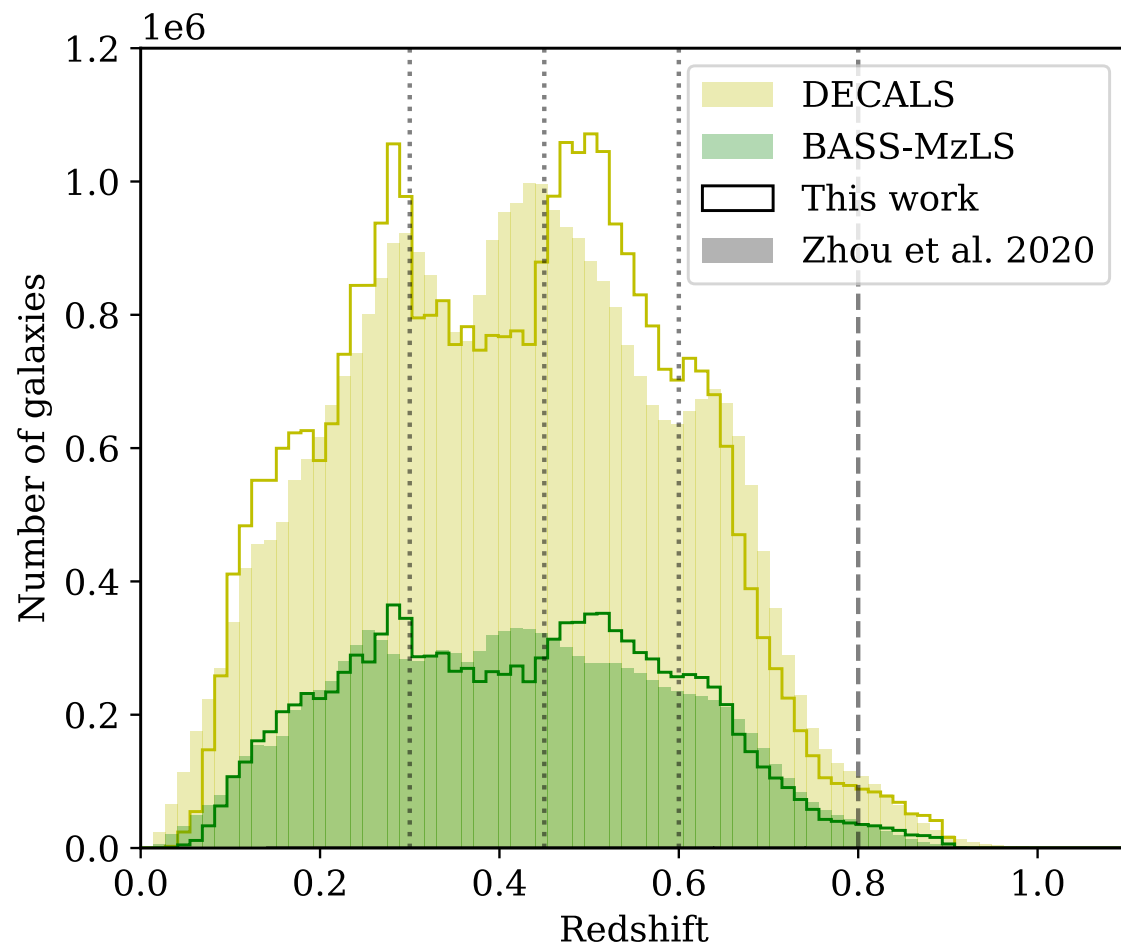
# 3. Calibration of the photometric redshifts

- Spectroscopic surveys are used to **calibrate** the redshift of Legacy Survey galaxies (GAMA, BOSS, eBOSS, VIPERS, DEEP2, COSMOS, DESY1A1 redMaGiC). These galaxies are matched in the Legacy Survey sample using their sky positions.
- Mean spec-z in **3D colour grids**: g-r, r-z, z-W1, with pixel width of  $\sim 0.03$ mag.



- We assign the mean redshifts in these grids to the Legacy Survey galaxies. Galaxies falling outside the grid covered by the calibration sample are excluded.
- **78.6%** of the selected Legacy Survey galaxies get assigned a photometric redshift.

# 3. Calibration of the photometric redshifts



- We also compare with the Zhou et al. (2020) machine-learning photometric redshift catalogue → select galaxies with  $|\Delta z| < 0.05$ .
- We split the sample into 4 tomographic bins in the redshift range  $0 < z < 0.8$ .

## Photo-z error

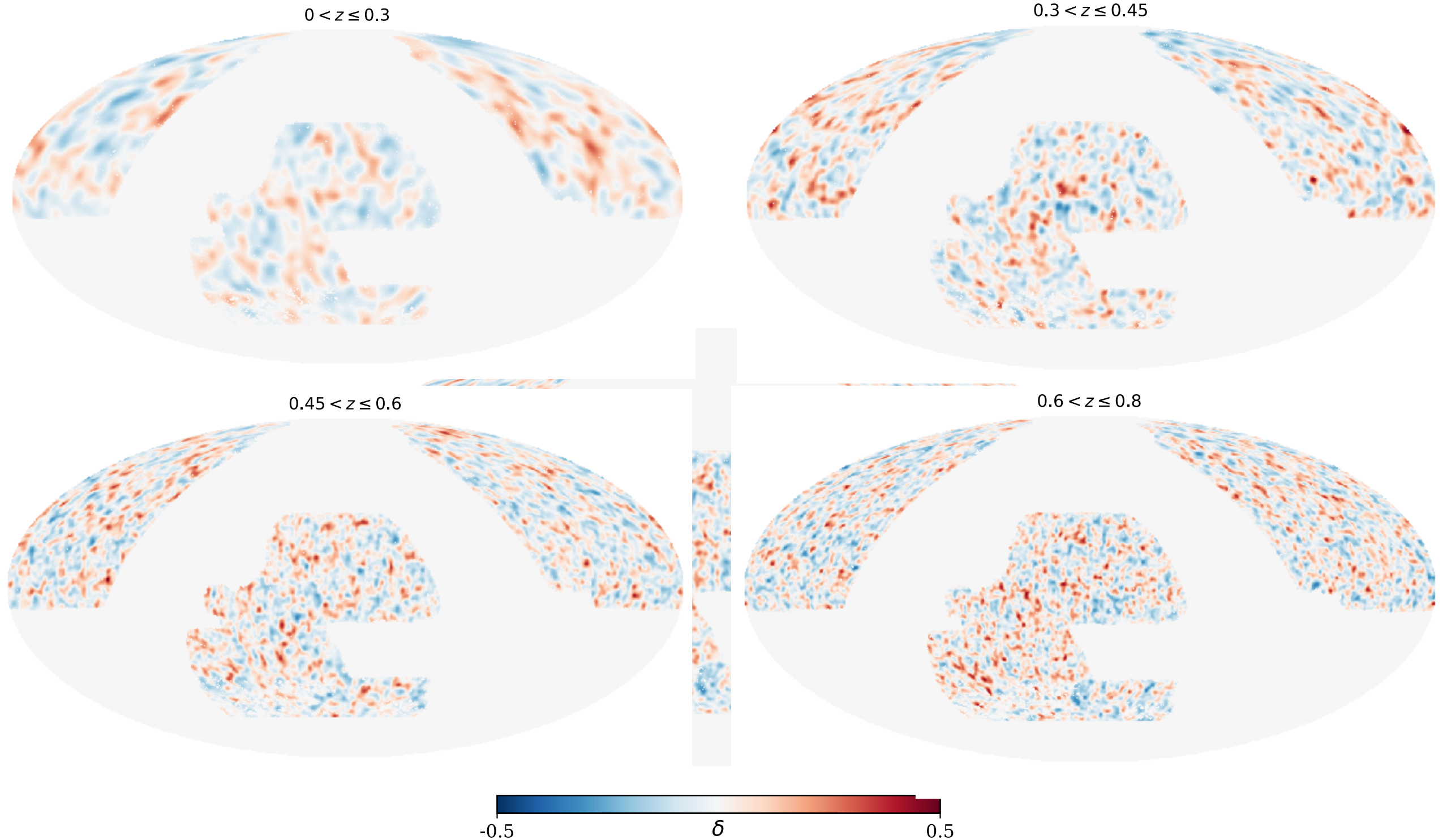
The raw redshift distribution is convolved with  $L(x)$  to obtain the final redshift distribution.

$$L(x) = \frac{N}{(1 + ((x - x_0)/\sigma)^2/2a)^a}$$

Normalization such that the integral is 1 (points to  $N$ )  
mean, free with constraint that sum of four bins is zero (points to  $x_0$ )  
width, fixed by fitting the spectroscopic sample in each  $z$  bin (points to  $\sigma$ )  
Tail, free to account for faint galaxies (points to  $a$ )

# Galaxy density maps

\*These density maps are smoothed with Gaussian kernel of width  $\sigma=20\text{Mpc}/h$ .



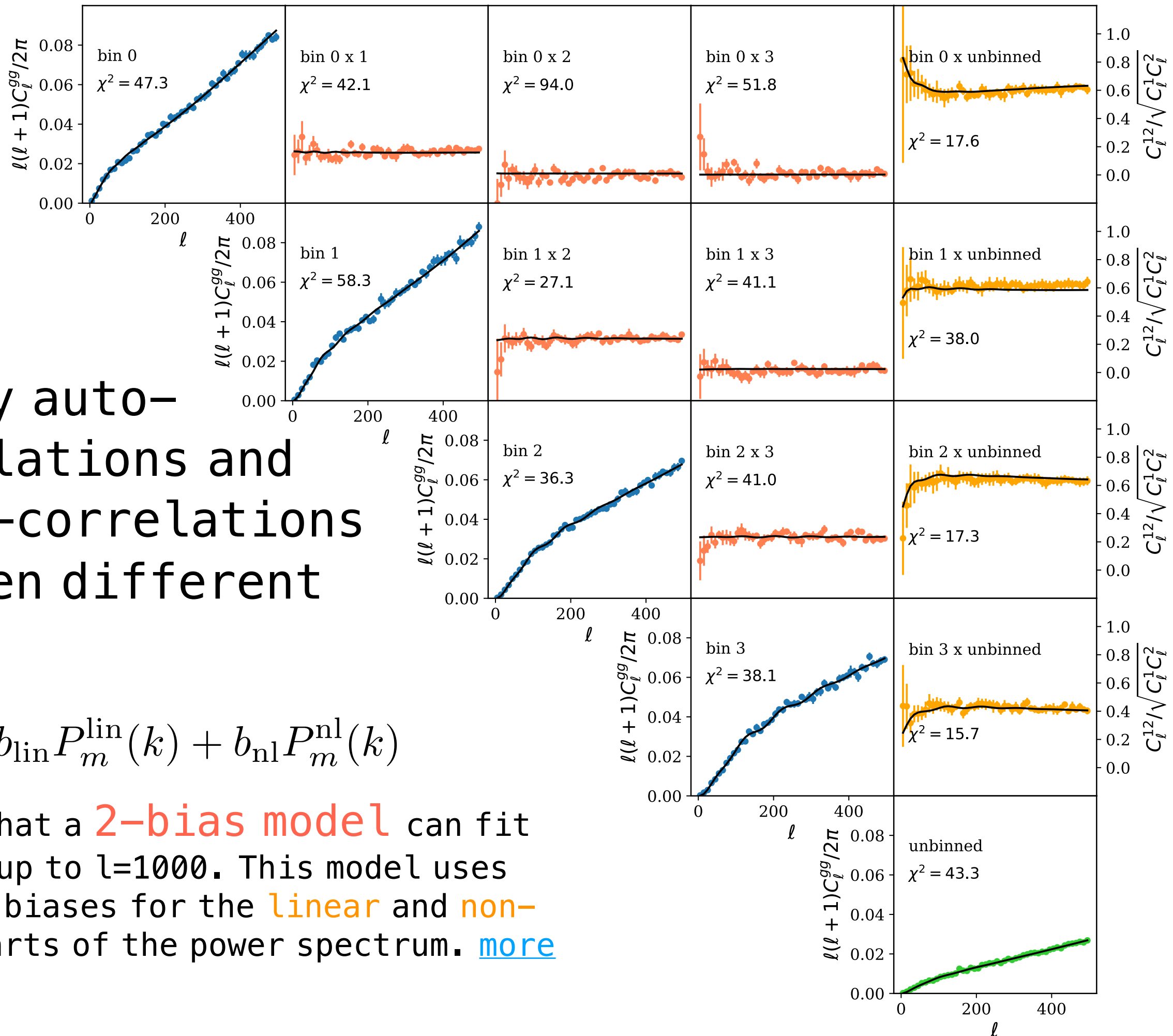
# 4. Cross-correlation Results and errors

- $l < 10$  modes are excluded from fitting.
- We use pseudo-power estimate  $\hat{C}_l = C_l^{\text{masked}} / f_{\text{sky}}$
- Use  $\Delta l = 10$  power bins. Covariance matrix then accurately diagonal (based on lognormal simulations). [more](#)
- Tomographic slices not completely independent. Use un-binned data for combined result.

# Galaxy auto- correlations and cross-correlations between different z bins

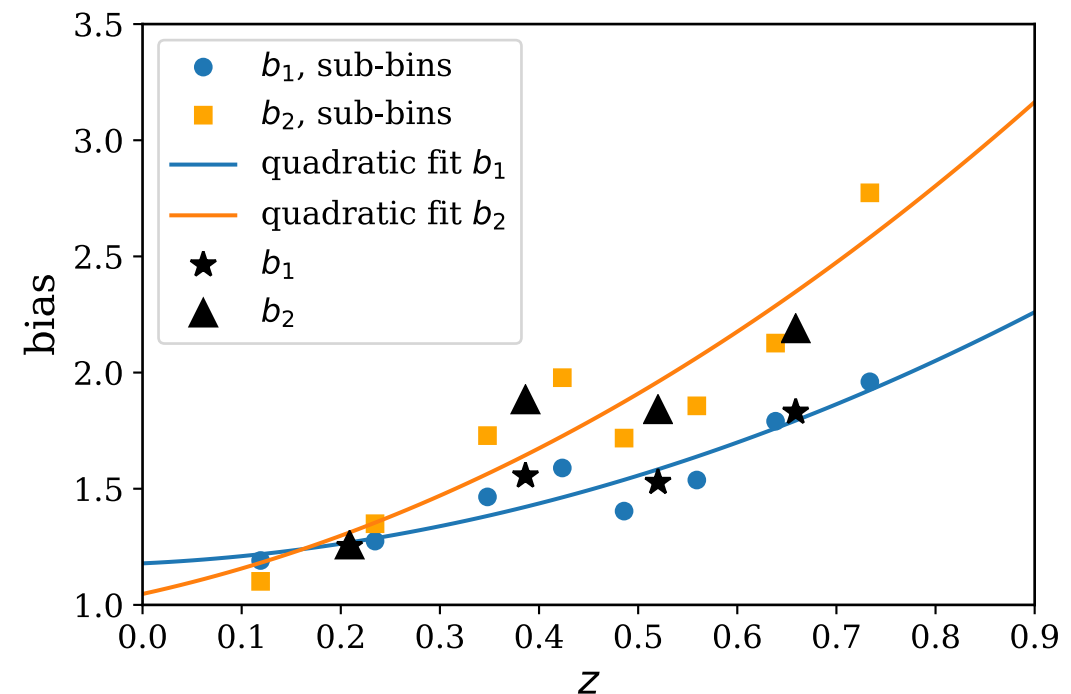
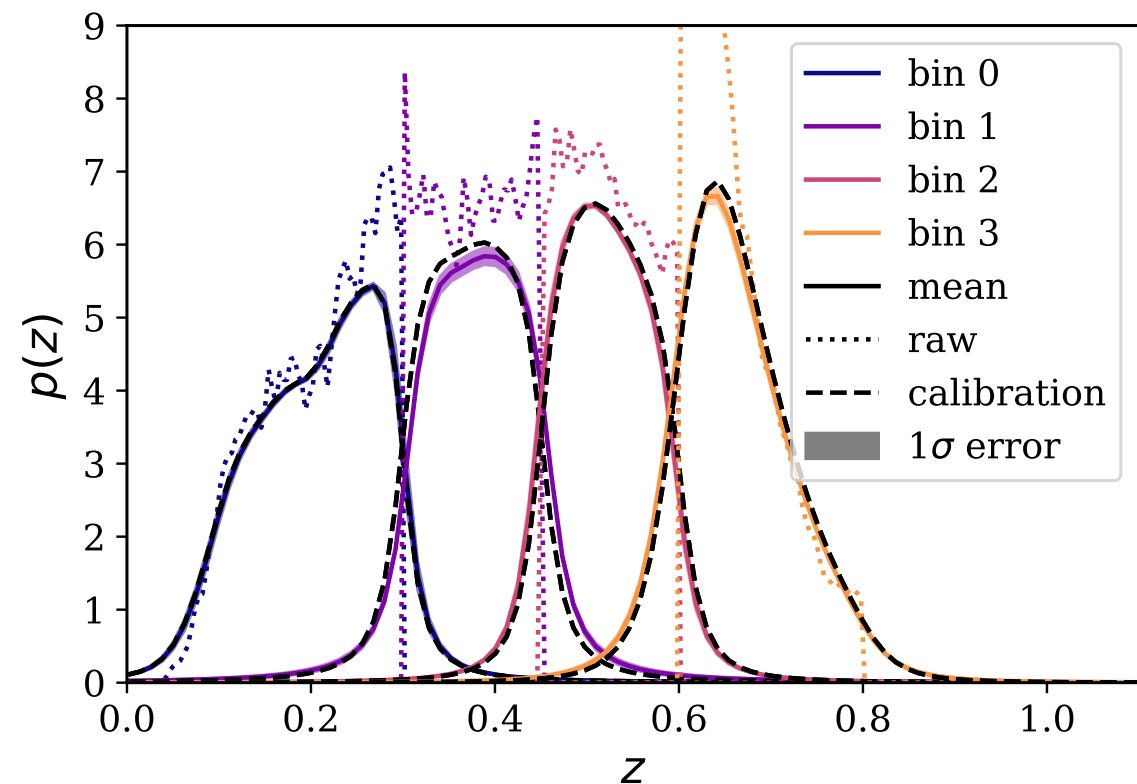
$$P_g(k) = b_{\text{lin}} P_m^{\text{lin}}(k) + b_{\text{nl}} P_m^{\text{nl}}(k)$$

We find that a **2-bias model** can fit the data up to  $l=1000$ . This model uses separate biases for the **linear** and **non-linear** parts of the power spectrum. [more](#)

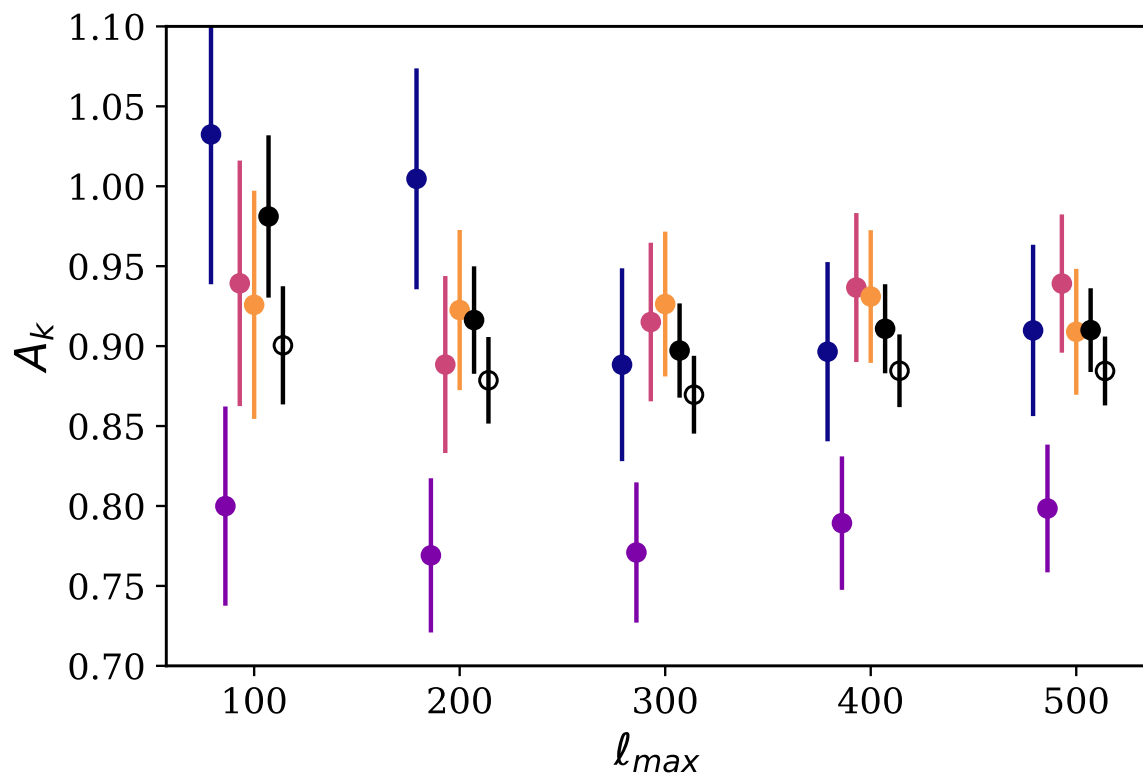
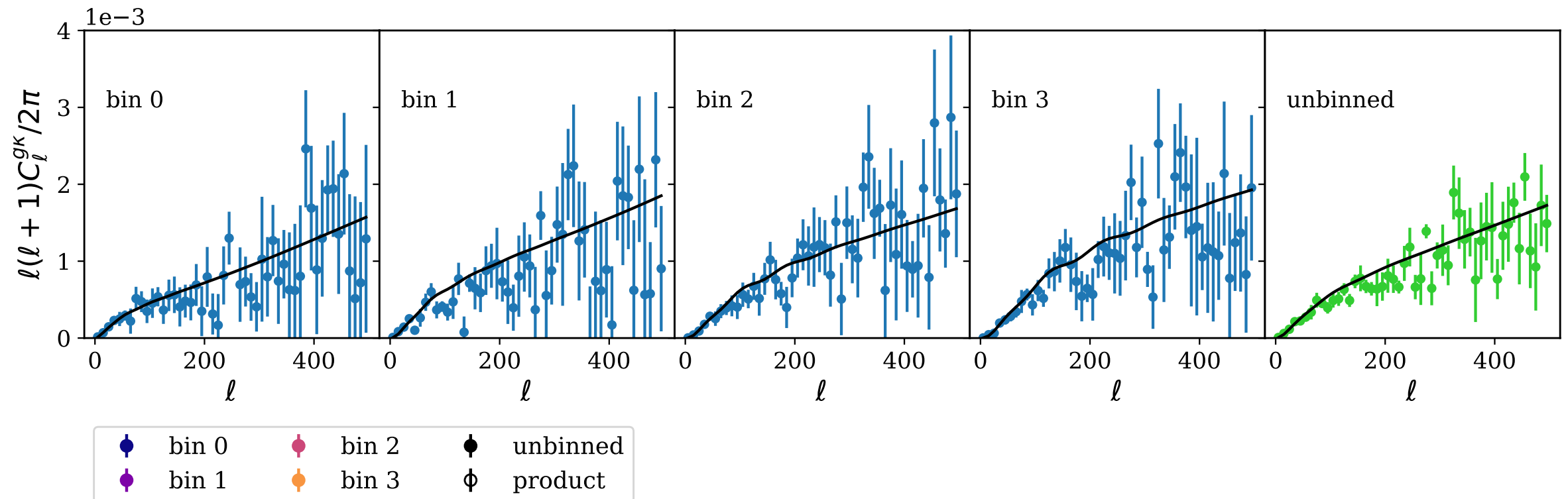


# Galaxy auto-correlations and cross-correlations between different $z$ bins

- We minimize the total chi square from the 10 galaxy correlations by varying photo- $z$  parameters. For each set of parameters, we fix bias at the lowest chi square value.
- For the combined bin case, we also further consider the **bias redshift evolution**, approximated via quadratic curve.
- The galaxy biases (and the evolution) are fixed for the CMB cross-correlation analysis.



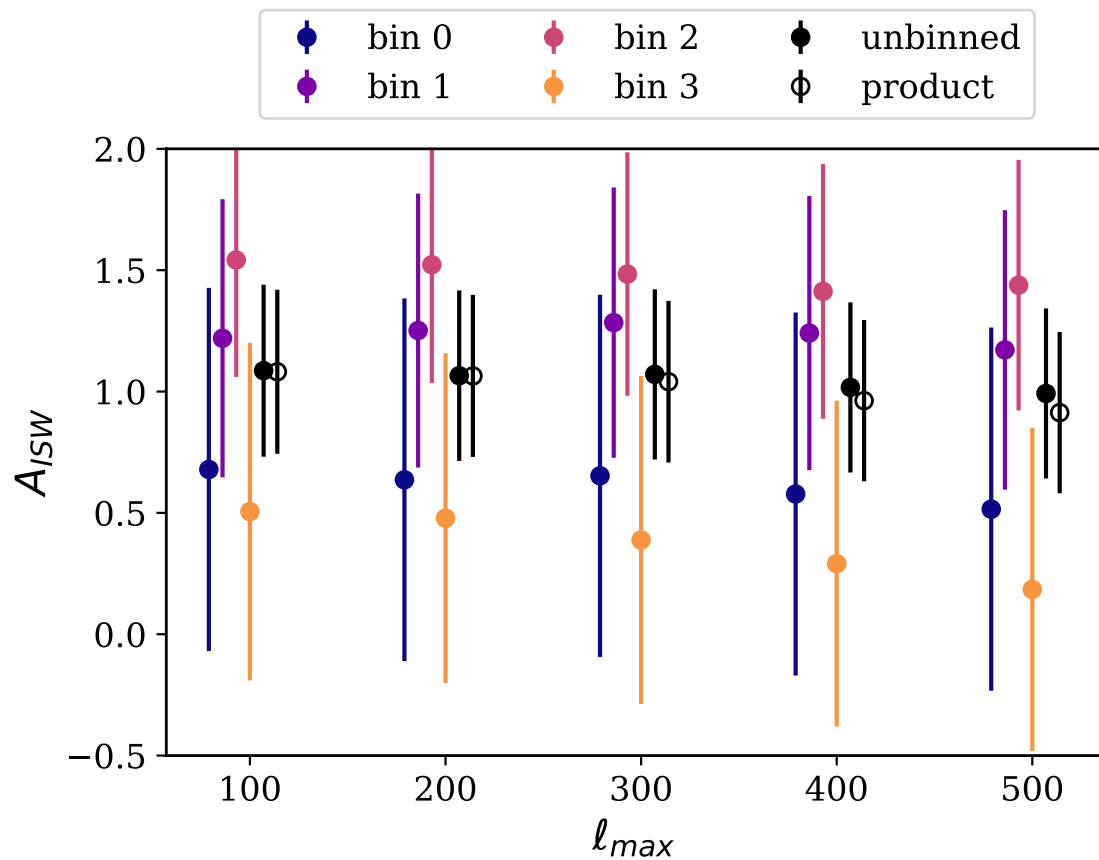
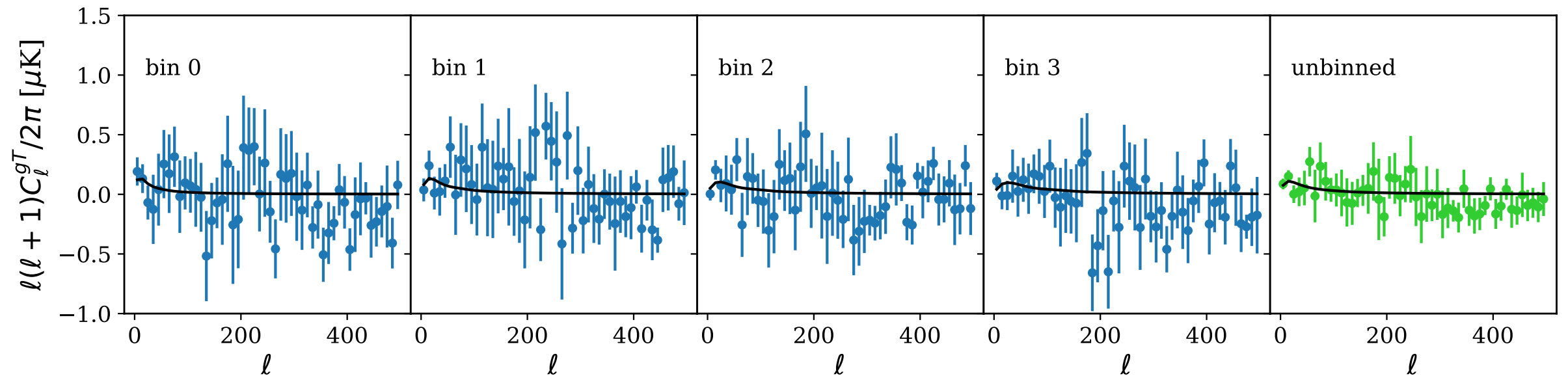
# Cross-correlations with the CMB maps – lensing results



The black lines are not fits to the data. We use  $A = \text{data}/\text{theory}$  to quantify the consistency between the two.  $A=1 \rightarrow$  fiducial cosmology is preferred. The result of combining the four redshift bins and the unbinned case both lie below unity.

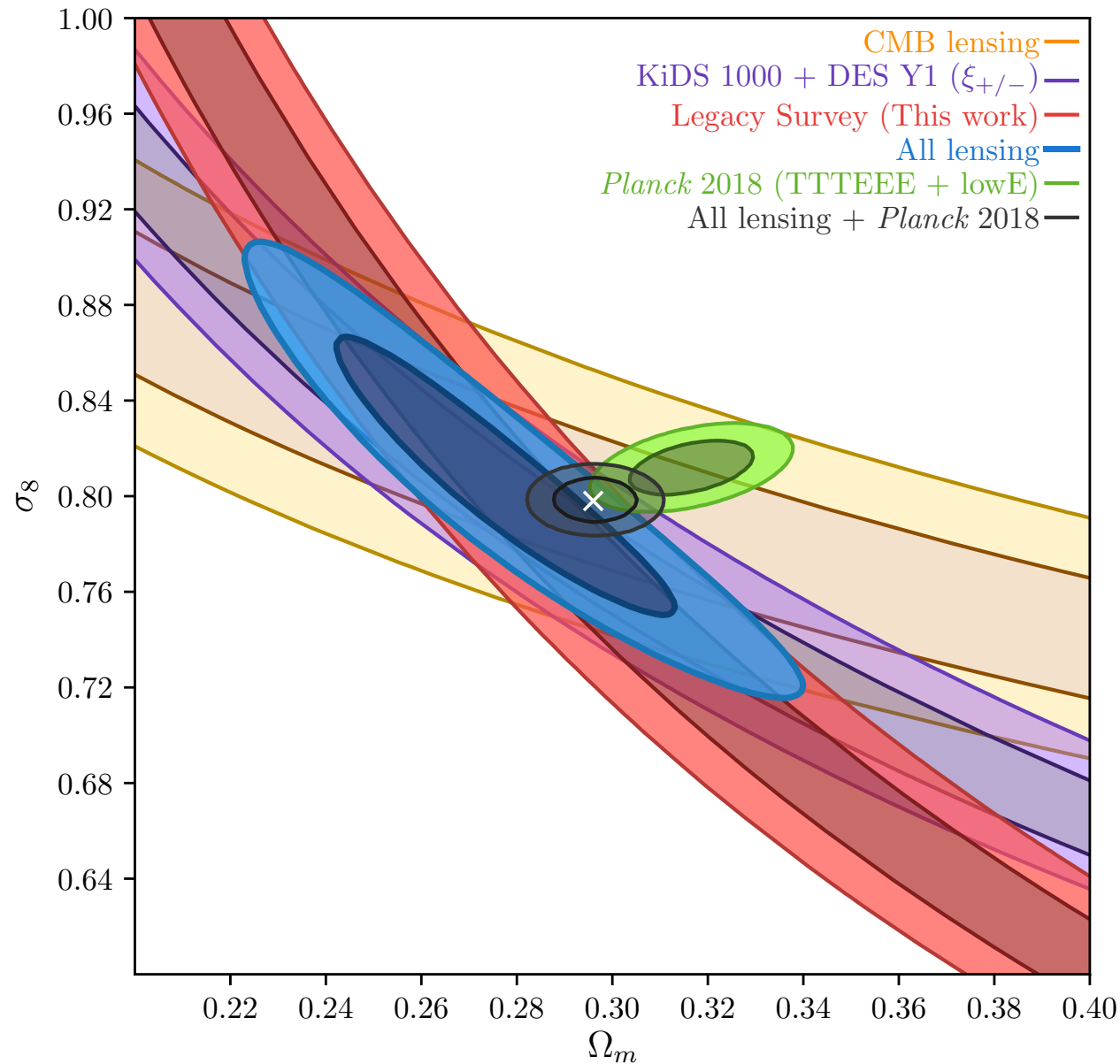
$$A_{\kappa} = 0.901 \pm 0.026$$

# Cross-correlations with the CMB maps – ISW results



- The ISW signal is very noisy.
- We find that  $A_{\text{ISW}} = 0.98 \pm 0.35$
- It is fully consistent with the fiducial cosmology given the large error bar. This consistency helps us rule out the **AvERA model** – a model which predicts much higher ISW signal in order to explain the excess signal in the **stacking results**.

# Cosmological implications of low $A_K$



- Tomographic galaxy–CMB lensing measures  $\sigma_8\Omega_m^{0.78}$ . Our results put a constraint on the quantity:  $\sigma_8\Omega_m^{0.78}=0.297\pm0.009$ . Total CMB lensing measures  $\sigma_8\Omega_m^{0.25}=0.589\pm0.020$ . In combination, we have  $\Omega_m=0.275\pm0.024$ ;  $\sigma_8=0.814\pm0.042$ .
- The other galaxy weak lensing experiments, **KiDS-1000** (Asgari et al. 2020) and **DES Y1** (Troxel et al. 2018) gives constraints which are consistent with ours, and in slight tension with **Planck**.
- Combination of **all lensing** results show  $\Omega_m=0.274\pm0.024$ ;  $\sigma_8=0.804\pm0.040$ . It seems that this prefers a lower  $\Omega_m$  than the Planck 2018 result.
- Everything combined:  $\Omega_m=0.296\pm0.006$ ;  $\sigma_8=0.798\pm0.006$ . The value is touching the 95% contour of both sets.

# Cosmological implications of low $A_K$

- Bad luck in statistics?
- Unknown systematics in galaxy data, e.g., photo-z, contamination...
- CMB side?
- Massive neutrinos? – the effect is negligible at low redshift. At Planck side, it increases the tension.
- Modified gravity? – to suppress growth of structure to achieve  $A_K=0.9$ , it needs substantial modification, which can be ruled out by other evidence such as RSD measurements.
- Modelling? [Kitanidis & White, 2020] found similar results with LRG using halofit, but not in perturbation theory.

# Cosmological implications of low $A_K$

There are also implications on the  $H_0$  tension...

Since the acoustic scale mainly fixes  $\Omega_m h^3$ , a lower  $\Omega_m$  needs higher  $h$ .

Our preferred  $\Omega_m=0.27$  would yield  $h=0.71$ , consistent with the local universe measurements from e.g., distance ladder.

# Summary

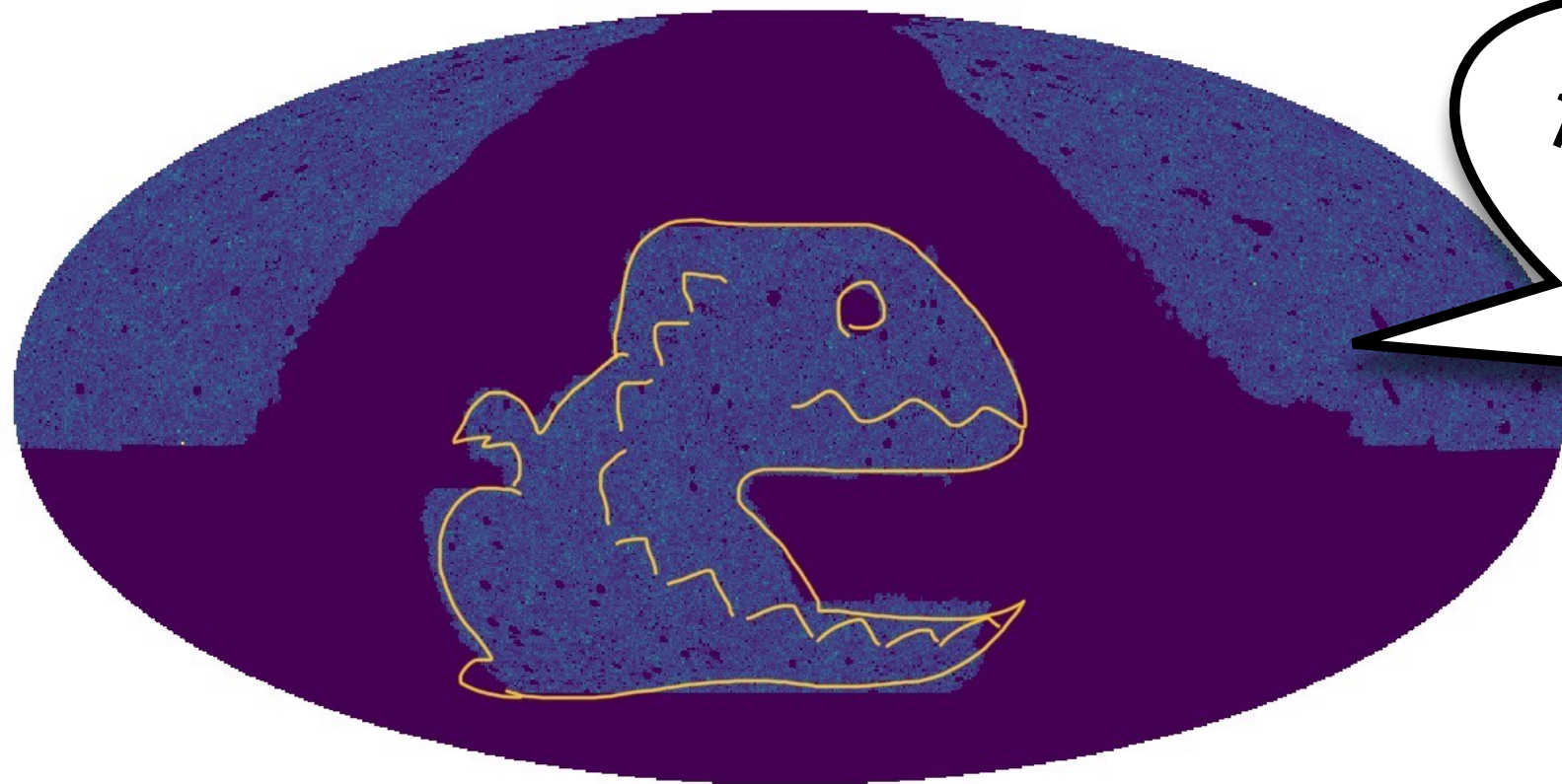
- We selected galaxies from the DESI Legacy Image Survey and obtained robust photometric redshifts using the available three colour bands.
- We constructed galaxy density maps for four tomographic bins between  $0 < z < 0.8$ .
- We measured the cross-correlation between these galaxy maps with the CMB lensing convergence and temperature maps.
- Compared with theoretical prediction based on Planck 2018 Cosmology, we find  $A_K = 0.901 \pm 0.026$  and  $A_{ISW} = 0.98 \pm 0.35$ .
- Our result translate to a strong evidence for lower  $\Omega_m$  combined other lensing probes.
- Future surveys such as DESI will no doubt provide more insight into this issue!

For more info: Q. Hang et al 2020, arXiv: 2010.00466

My other ongoing works:

Stacking of super structures in the Legacy Survey with CMB  
[Q. Hang et al. in prep.]

RSD from group-galaxy cross-correlation using GAMA [Q.  
Hang et al. in prep.]



Available  
for postdocs from  
mid-2021

# Modelling the signal

$$\frac{\ell(\ell+1)}{2\pi} C_\ell^{gX} = \frac{\pi}{\ell} \int b \Delta^2(k = \ell/r, z) p(z) K^X(z) r dz$$

galaxy bias

matter power spectrum

redshift distribution

X=Lensing  $K^\kappa = \frac{3H_0^2 \Omega_m}{2c^2 a} \frac{r(r_{\text{LS}} - r)}{r_{\text{LS}}}$

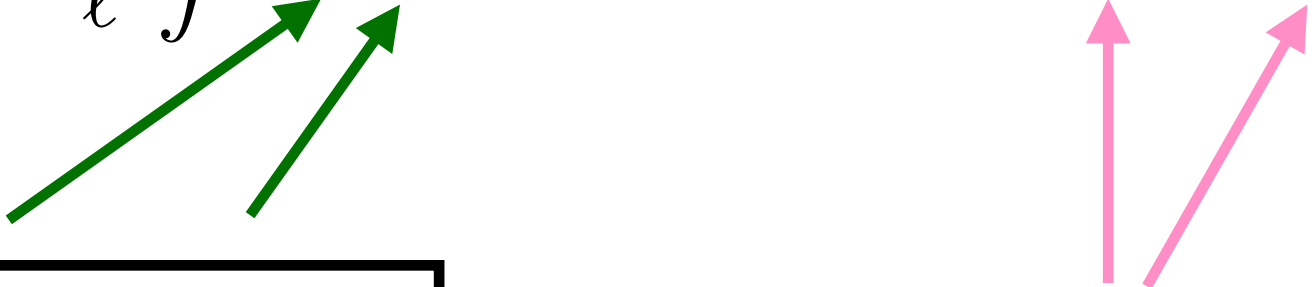
X=ISW Assume linear theory,  $\Phi = \frac{3H_0^2 \Omega_m}{2ak^2} \delta$

$$K^T = \frac{2T_{\text{CMB}}}{c^3} \frac{3H_0^2 \Omega_m}{2k^2} H(z) (1 - f_g(z))$$

growth rate

# Theory: galaxy–galaxy auto/ cross–correlations

Galaxy bias and redshift distribution can be constrained from the galaxy–galaxy correlations, given fixed cosmology.

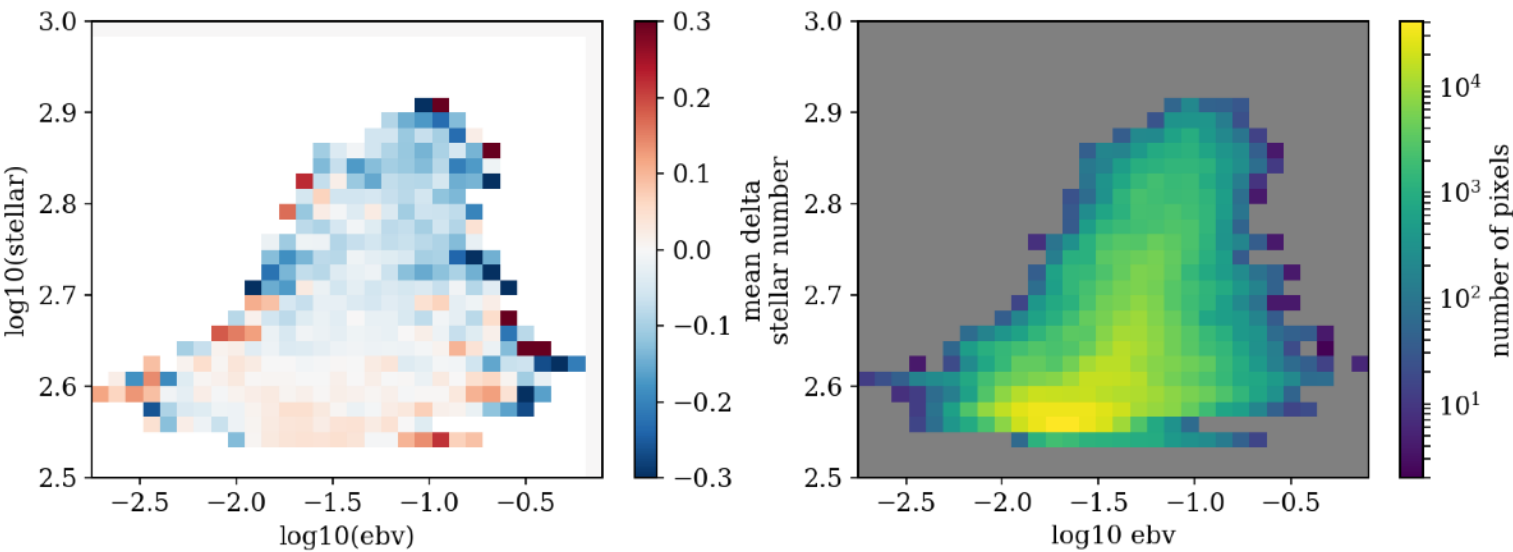
$$\frac{\ell(\ell + 1)}{2\pi} C_{\ell}^{gg} = \frac{\pi}{\ell} \int b_1 b_2 \Delta^2(k = \ell/r, z) p_1(z) p_2(z) \frac{H(z)r}{c} dz$$


In principle, the galaxy bias can have redshift and scale dependence.

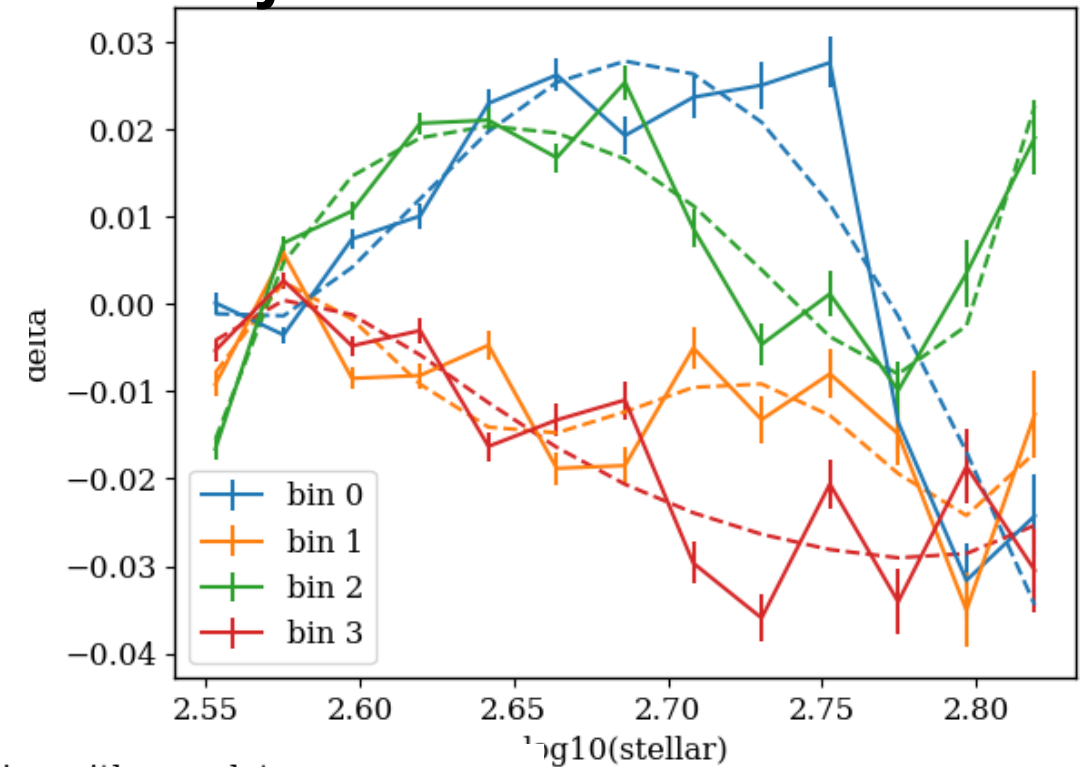
$p_1=p_2 \rightarrow$  auto–correlation,  
 $p_1 \neq p_2 \rightarrow$  cross–correlation between different redshift slices.

# Density map systematic correction

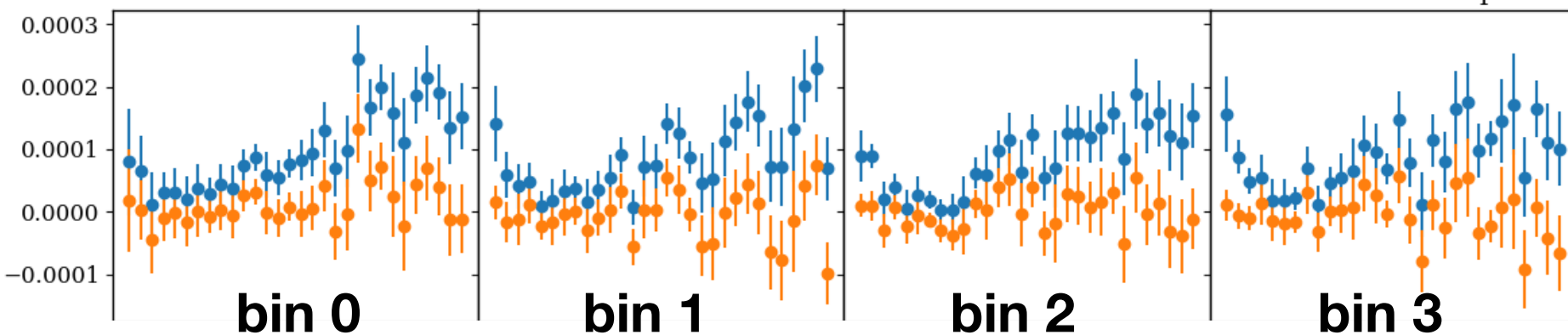
Mean density split in bins of stellar number and E(B-V)



Density variation with stellar density

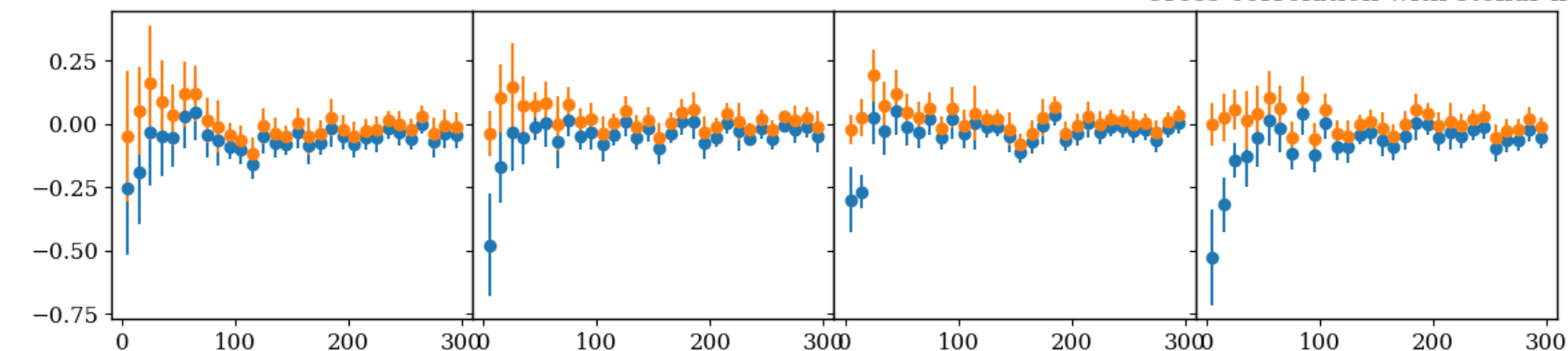


Cross-correlation with completeness map



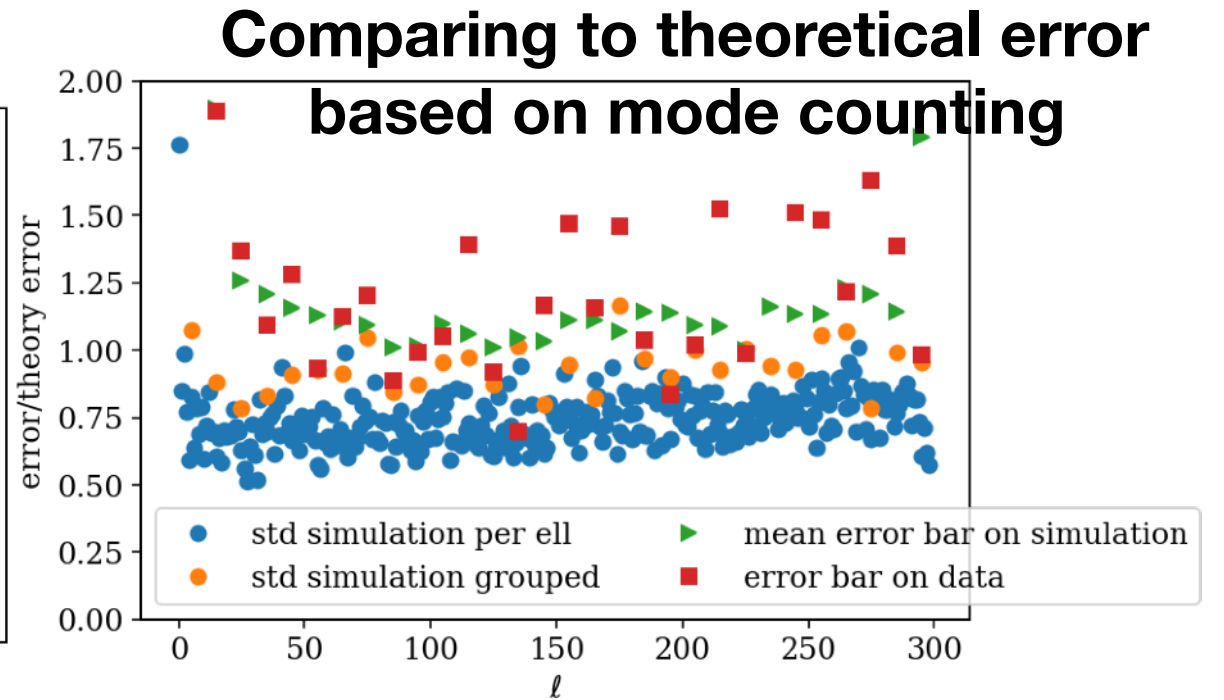
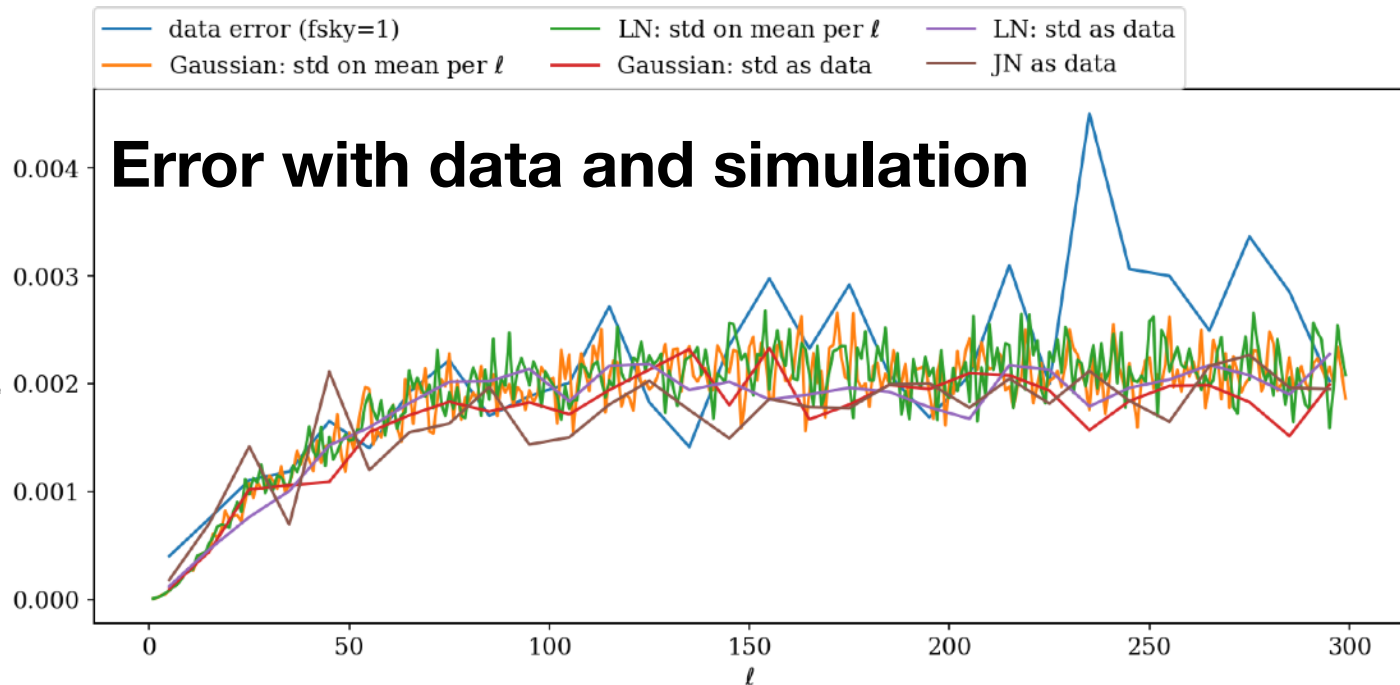
— Before weighting and stellar correction

Cross-correlation with stellar map

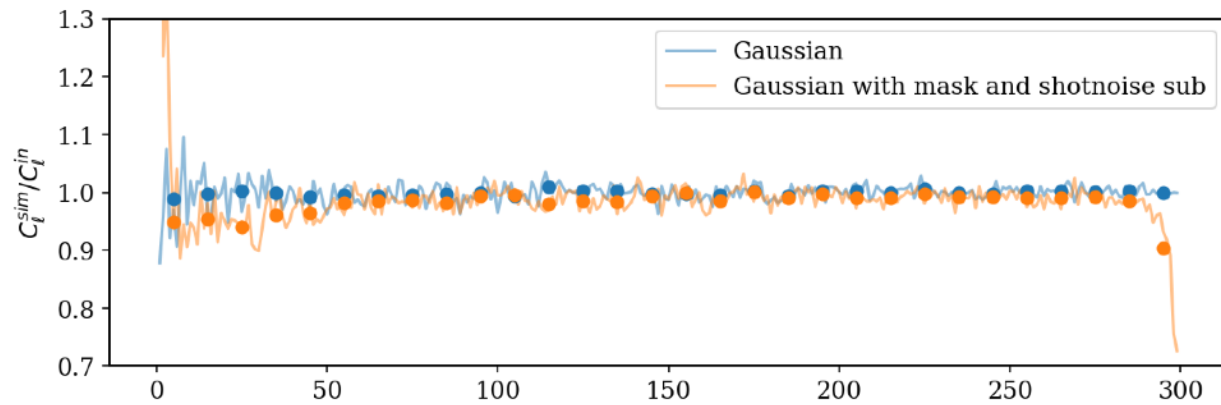


— Weighted by completeness and corrected by stellar density

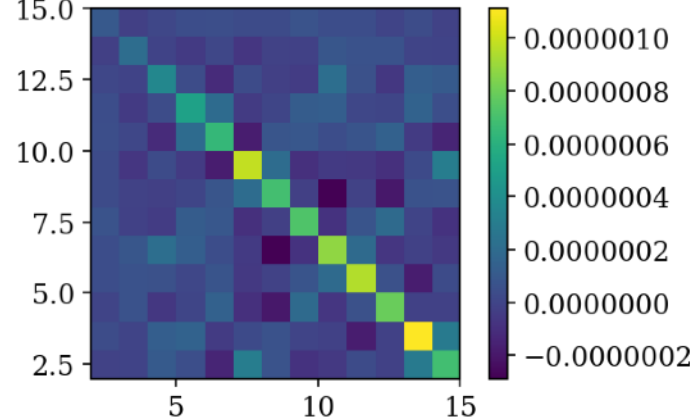
# Mask, shotnoise, errorbars



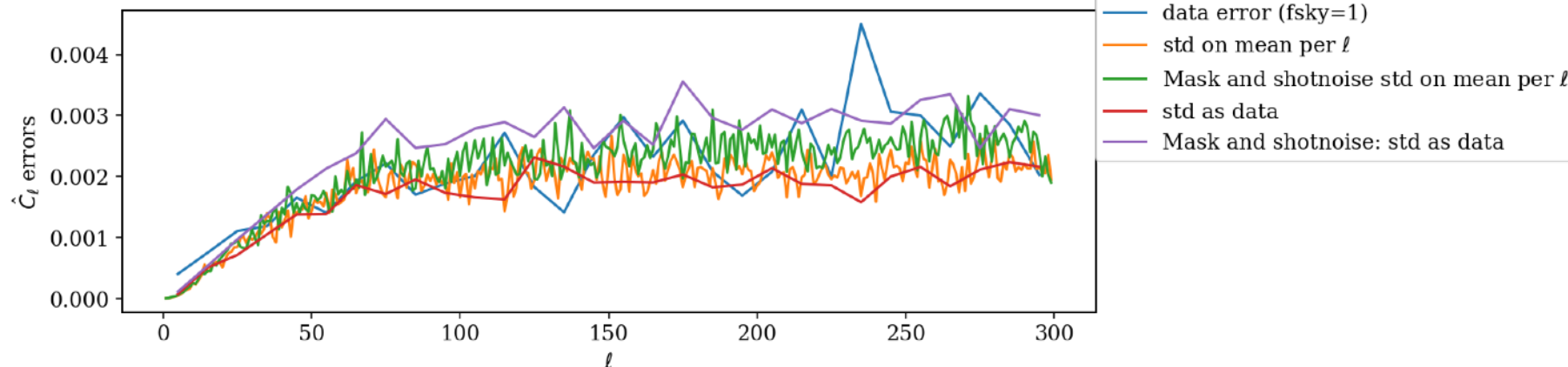
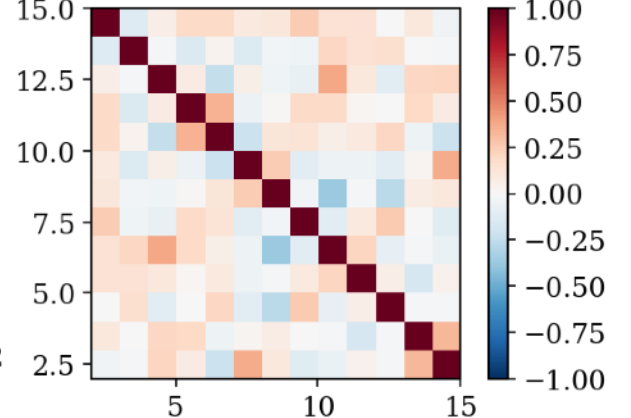
## Including mask and shot noise



Covariance matrix

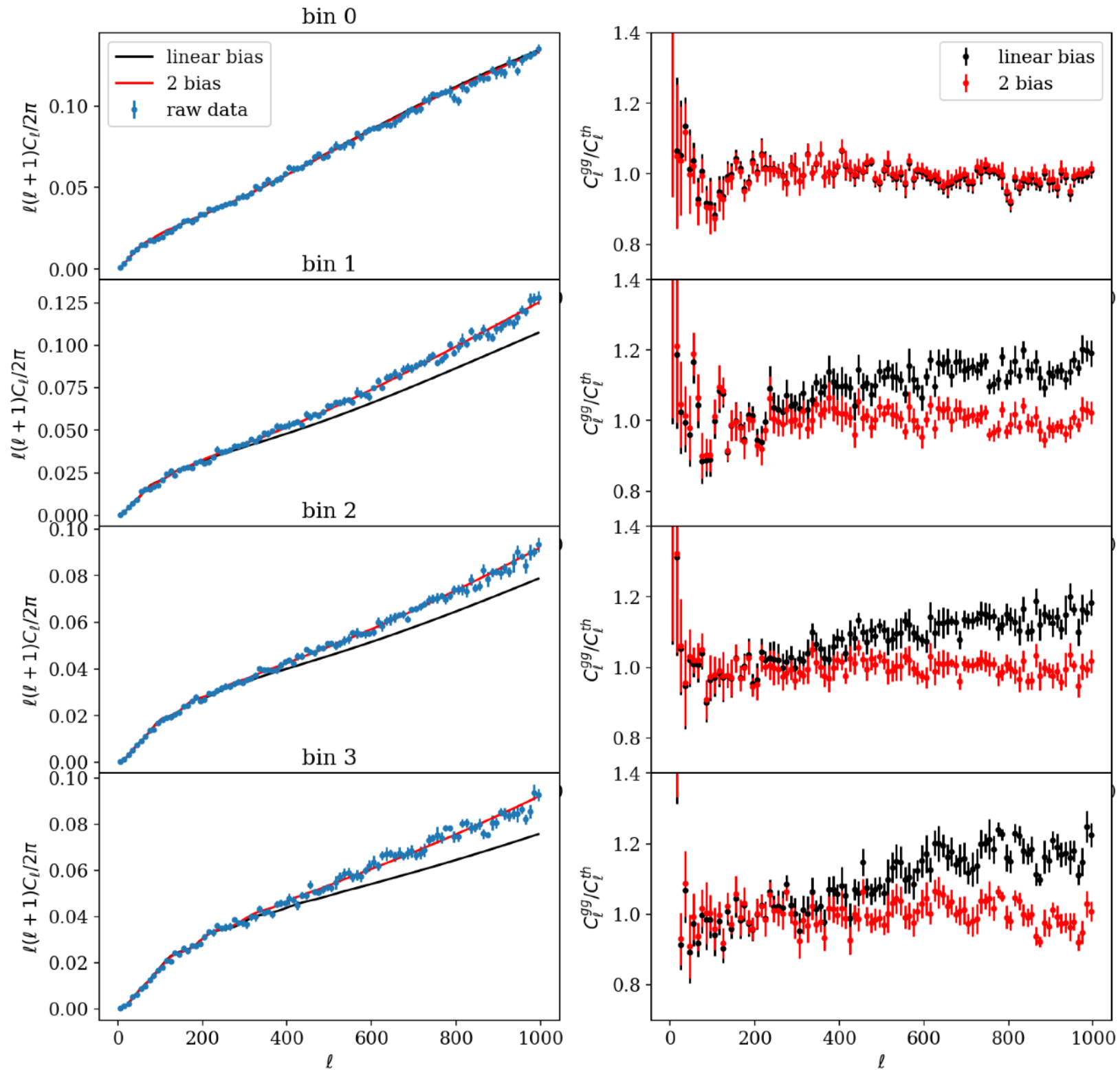


Correlation matrix



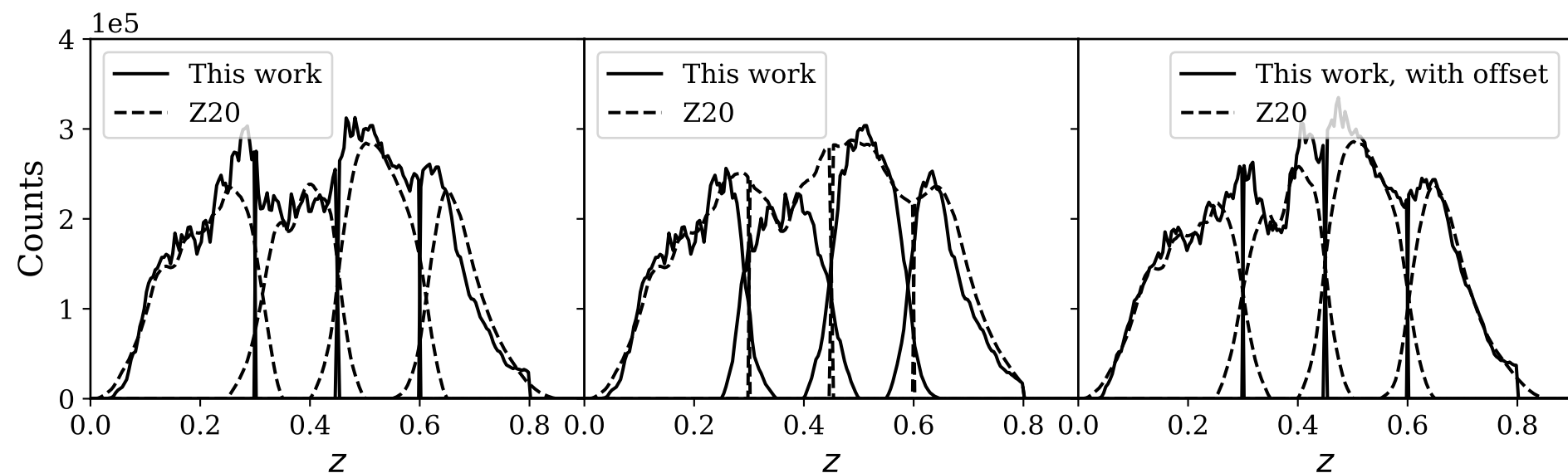
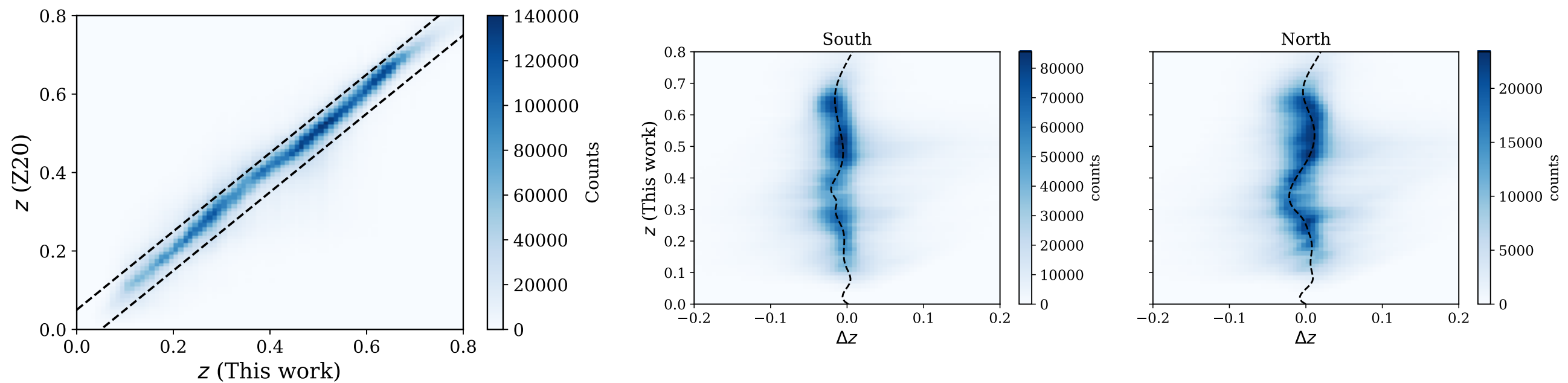
**Covariance from 50 simulations for modes between  $10 < l < 150$ , with mask and shot noise.**

# 2-bias model

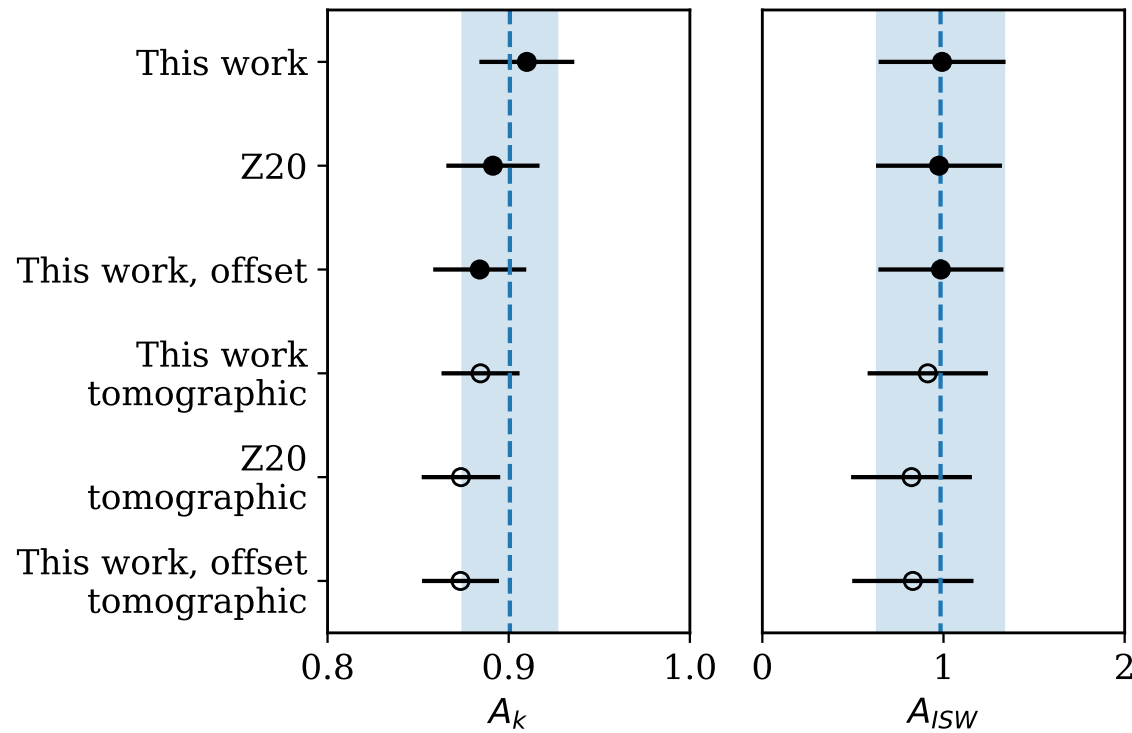


**The ratio between data and model with a constant bias show a change at transition between linear and non-linear scales. The ratio on either end of the scales seem flat.**

# Comparison between our photo- z and [Zhou et. al. 2020]



# Systematic tests



| Parameters                                 | bin0             | bin1                | bin2                | bin3               | combined        | Un-binned        |
|--|------------------|---------------------|---------------------|--------------------|-----------------|------------------|
| Redshift                                   | $0 < z \leq 0.3$ | $0.3 < z \leq 0.45$ | $0.45 < z \leq 0.6$ | $0.6 < z \leq 0.8$ | -               | $0 < z \leq 0.8$ |
| <b>Marginalized over <math>p(z)</math></b> |                  |                     |                     |                    |                 |                  |
| $b_1$                                      | $1.25 \pm 0.01$  | $1.53 \pm 0.02$     | $1.54 \pm 0.01$     | $1.86 \pm 0.02$    | -               | -                |
| $b_2$                                      | $1.27 \pm 0.01$  | $1.85 \pm 0.03$     | $1.82 \pm 0.01$     | $2.23 \pm 0.02$    | -               | -                |
| $A_k$                                      | $0.91 \pm 0.05$  | $0.82 \pm 0.04$     | $0.94 \pm 0.04$     | $0.90 \pm 0.04$    | $0.89 \pm 0.02$ | -                |
| $A_{ISW}$                                  | $0.52 \pm 0.78$  | $1.20 \pm 0.63$     | $1.48 \pm 0.61$     | $0.18 \pm 0.67$    | $0.91 \pm 0.33$ | -                |
| <b>Best-fit <math>p(z)</math></b>          |                  |                     |                     |                    |                 |                  |
| $b_1$                                      | 1.25             | 1.56                | 1.53                | 1.83               | -               | 1.43             |
| $b_2$                                      | 1.26             | 1.88                | 1.84                | 2.19               | -               | 1.59             |
| $A_k$                                      | $0.91 \pm 0.05$  | $0.80 \pm 0.04$     | $0.94 \pm 0.04$     | $0.91 \pm 0.04$    | $0.88 \pm 0.02$ | $0.91 \pm 0.03$  |
| $A_{ISW}$                                  | $0.52 \pm 0.75$  | $1.17 \pm 0.58$     | $1.44 \pm 0.52$     | $0.18 \pm 0.67$    | $0.91 \pm 0.33$ | $0.99 \pm 0.35$  |
| <b>Zhou et. al.</b>                        |                  |                     |                     |                    |                 |                  |
| $b_1$                                      | 1.25             | 1.54                | 1.55                | 1.90               | -               | 1.44             |
| $b_2$                                      | 1.26             | 1.87                | 1.90                | 2.21               | -               | 1.62             |
| $A_k$                                      | $0.91 \pm 0.06$  | $0.81 \pm 0.04$     | $0.93 \pm 0.04$     | $0.87 \pm 0.04$    | $0.87 \pm 0.02$ | $0.89 \pm 0.03$  |
| $A_{ISW}$                                  | $0.50 \pm 0.79$  | $1.03 \pm 0.59$     | $1.37 \pm 0.55$     | $0.20 \pm 0.63$    | $0.82 \pm 0.33$ | $0.98 \pm 0.35$  |
| <b>Offset</b>                              |                  |                     |                     |                    |                 |                  |
| $b_1$                                      | 1.28             | 1.52                | 1.54                | 1.89               | -               | 1.45             |
| $b_2$                                      | 1.30             | 1.86                | 1.87                | 2.20               | -               | 1.64             |
| $A_k$                                      | $0.89 \pm 0.05$  | $0.81 \pm 0.04$     | $0.93 \pm 0.04$     | $0.89 \pm 0.04$    | $0.87 \pm 0.02$ | $0.88 \pm 0.03$  |
| $A_{ISW}$                                  | $0.45 \pm 0.81$  | $1.05 \pm 0.58$     | $1.32 \pm 0.56$     | $0.25 \pm 0.46$    | $0.83 \pm 0.33$ | $0.99 \pm 0.35$  |
| <b>AvERA model</b>                         |                  |                     |                     |                    |                 |                  |
| $b_1$                                      | 1.16             | 1.34                | 1.25                | 1.46               | -               | 1.23             |
| $b_2$                                      | 1.11             | 1.50                | 1.45                | 1.75               | -               | 1.33             |
| $A_k$                                      | $0.97 \pm 0.06$  | $0.80 \pm 0.04$     | $0.91 \pm 0.04$     | $0.85 \pm 0.04$    | $0.87 \pm 0.02$ | $0.91 \pm 0.03$  |
| $A_{ISW}$                                  | $0.24 \pm 0.35$  | $0.48 \pm 0.25$     | $0.55 \pm 0.23$     | $0.07 \pm 0.24$    | $0.35 \pm 0.13$ | $0.39 \pm 0.14$  |